Real-Time Economic Dispatch for Integrated Energy Microgrid Considering Ancillary Services

Yanling Lin*†, Xiaohu Zhang*, Shengfei Yin†, Jianhui Wang† and Di Shi*
*GEIRI North America, San Jose, CA, USA
†Southern Methodist University, Dallas, TX, USA
Email:yanlingl, gyin, jianhui@mail.smu.edu
xiaohu.zhang, di.shi@geirina.net

***Abstract*—An integrated energy microgrid (IEM) system consists of power, natural gas, and heat. As the interdependence among different energy utilities grows, there is an urgent need to investigate the combined economic dispatch of the IEM. This paper proposes a convex real-time economic dispatch model for a grid-connected IEM considering ancillary services from diverse resources. The power and gas system models are relaxed by second-order cone programming (SOCP), and the cost function and feasible region of the combined heat and power (CHP) unit are linearly approximated. The effectiveness of the proposed method is verified in the case studies. The cost-effectiveness of enabling energy storage systems (ESSs) to provide ancillary services is demonstrated.**

***Index Terms*—Integrated energy system, economic dispatch, ancillary services.**

I. Introduction

The energy crisis and environmental challenges are driving the need for more efficient planning and operation of the energy system [1], [2]. An integrated energy microgrid (IEM) is an efficient solution to strengthen the interaction of multiple energy systems, which includes electricity, natural gas, and heat.

The economic dispatch of an IEM is highly complex due to the non-convexity from the individual system models. These complexities pose even more significant challenges to the system operators in the real-time scale, which calls for faster and more accurate solutions. Compared with the widely applied linearized energy flow models, second-order cone programming (SOCP) based energy flow models have the potential to provide more accurate results for real-time economic dispatch (RTED). Existing research works have tackled the SOCP relaxation for single-phase balanced power distribution systems [3] and natural gas systems [4]. For the coordination with the heat system, the research focuses on the approximated heat model, such as the variable-temperature constant-flow (VT-CF) model [5]. Currently, there lacks an efficient RTED model that simultaneously considers the power, natural gas, and heat.

During the RTED scheduling interval, ancillary services are required to follow the moment-to-moment differences between generation and demand. Traditionally, thermal generators in a power system are the major provider of ancillary services, including primary frequency responses (PFR), automatic generation control (AGC)-up, and AGC-down services. On the other hand, because energy storage systems (ESSs) have better ramping characteristics than thermal generators, their contribution to the ancillary services should not be ignored. Ref. [6] investigates the participation of ESSs in the frequency regulation services. Ref. [7] proposes a joint optimization framework for ESSs to perform peak shaving and provide frequency regulation services. Currently, the integration of ancillary services in the RTED for multi-energy systems still awaits more in-depth investigation concerning the coordination of non-gas generators, gas-fired generators, combined heat and power (CHP) and ESSs.

This paper proposes a RTED framework for grid-connected IEM. The major contribution of this paper is a) the SOCP-based power and gas flow models, with a linearized approximation of the CHP model for IEM; b) the availability constraint formulation for PFR and AGC services from diverse resources, including distributed generators (DG) and ESSs. The rest of the paper is organized as follows. Section II describes the proposed method; section III tests the proposed method, and section IV concludes the paper.

This work is supported by SGCC Science and Technology Program under project Hybrid Energy Storage Management Platform for Integrated Energy System.

II. Mathematical Formulation

This section presents a rolling-horizon RTED model. The inputs include the unit commitment schedule, demand forecast, forecast of intermittent resources, etc. The objective of RTED is to minimize the operation cost of the IEM while satisfying the real-time energy demand.

A. Objective function

The objective function of the proposed model is provided in (1). It minimizes the total operation cost at time t for the next T intervals, which includes cost/revenue from energy transactions with the main grid, cost from non-gas DG, charging/discharging costs of ESSs, demand response, PFR and AGC shortage penalty, line loss, gas procurement, gas energy storage (GES) cost, and CHP cost. q with different superscripts indicates prices, e.g. $q_{buy,t}^{LMP}$ is the price buying energy from the main grid, $q_{sell,t}^{LMP}$ price selling to the main grid, q_s^{ESS} charging/discharging cost of ESS. $f_g()$ is the piecewise linearized cost function of non-gas DG; $f_{cp}()$ is the

convex cost function of CHP that can be linearly approximated by the method from [5].

$$Min \sum_{t}^{T}[q_{buy,t}^{LMP}P_{buy,t} - q_{sell,t}^{LMP}P_{sell,t} + \sum_{NG} f_g(P_{g,j,t}) + \sum_{ESS} q_s^{ESS}(P_{ch,s,t} + P_{dis,s,t}) + q_t^{DR}DR_t + q_t^{P}PFR_t^{short} + q_t^{A}(AGC_{up,t}^{short} + AGC_{down,t}^{short}) + q^{l}\sum_{l} R_l l_{l,t} + \sum_{GR} q_{gr,t}^{gas} g_{gr,t} + \sum_{GES} q_s^{GES}(g_{ch,s,t} + g_{dis,s,t}) + \sum_{CHP} f_{cp}(p_{h,t}, h_{h,t})]\Delta T \tag{1}$$

B. Energy Storage

For the ESS and GES s, we present the prevalent linear energy system formulation (2)-(5), where $SOC_{s,t}$ is the state of charge, $P_{ch,s,t}$ and $P_{dis,s,t}$ are the charging/discharging power, E_{C_s} is the energy capacity, η is the charge/discharging efficiency; λ indicates the charging stage, and $\lambda = 0$ means that the storage is in the discharging stage. This model is suitable for ESS that does not provide ancillary services. The model for ESS providing ancillary services is presented in the next section.

$$SOC_s^{min} \leq SOC_{s,t} \leq SOC_s^{max} \tag{2}$$

$$Dis_s^{min} \cdot (1 - \lambda_{s,t}) \leq P_{dis,s,t}/\eta \leq Dis_s^{max} \cdot (1 - \lambda_{s,t}) \tag{3}$$

$$Chi_s^{min} \cdot \lambda_{s,t} \leq P_{ch,s,t} \cdot \eta \leq Chi_s^{max} \cdot \lambda_{s,t} \tag{4}$$

$$SOC_{s,t} = SOC_{s,t-1} + \Delta T/E_{C_s}(P_{ch,s,t} \cdot \eta - P_{dis,s,t}/\eta) \tag{5}$$

C. Ancillary services

In this paper, we assume that all the online DG, CHP and ESSs can provide ancillary services. Therefore, in the RTED process, it is critical to manage the deployment availability of these resources. If a resource is scheduled to provide ancillary resources, it should be available to be deployed and provide the corresponding services in real-time operation. As the scheduling model only considers capacity-based requirements, it does not incorporate the speed of these services. For DG i, assume that $P_{g,i,t}$ is the output; $PFR_{i,t}$, $AGC_{i,t}^{up}$ and $AGC_{i,t}^{down}$ are the ancillary services. The DG uses its headroom to provide PFR. Constraints (6) and (7) describe the contribution of each DG providing PFR capacity and its sensitivity to frequency, the Δf^{max} is maximum frequency deviation, DB_i is the DG's governor dead band, and the R_i^{eq} is the equivalent droop. $I_{i,t}$ is the unit commitment status.

$$PFR_{i,t} \leq \frac{\Delta f^{max} - DB_t}{R_g^{eq}} \tag{6}$$

$$P_{g,i,t} + PFR_{i,t} \leq I_{i,t} \cdot P_{g,i,t}^{max} \tag{7}$$

PFR and AGC work at different time scales, and the availability constraints for PFR and AGC are therefore decoupled. For the AGC-up and AGC-down services, they have to satisfy the DG output capacity (8)-(9). The availability of AGC is also constrained by ramp rate: (10)-(13). T_{rec} is the maximum allowed frequency recovery time.

$$P_{g,i,t} + AGC_{i,t}^{up} \leq I_{i,t} \cdot P_{g,i,t}^{max} \tag{8}$$

$$P_{g,i,t} - AGC_{i,t}^{down} \geq I_{i,t} \cdot P_{g,i,t}^{min} \tag{9}$$

$$AGC_{i,t}^{up} \leq Ramp_i \cdot T_{rec} \tag{10}$$

$$AGC_{i,t}^{down} \leq Ramp_i \cdot T_{rec} \tag{11}$$

$$P_{g,i,t} + AGC_{i,t}^{up} - P_{i,t-1} \leq Ramp_i \tag{12}$$

$$P_{g,i,t} - AGC_{i,t}^{up} - P_{i,t-1} \geq -Ramp_i \tag{13}$$

ESSs are an essential part of an IEM with renewable energy. The fast ramping and flexibility of ESSs make them a great candidate to provide ancillary services. To enable ESSs to provide ancillary services, based on [7], the charging/discharging power of ESSs can be divided into two parts: one part is related with the market, and the other part is related with the ancillary services. For example, $P_{dis,s,t}$ is divided into $P_{dis,s,t}^{Energy}$ and $PFR_{s,t}$. The PFR and AGC constraints for ESSs are: (3)(14)-(20).

$$P_{dis,s,t}^{Energy} + PFR_{s,t} \leq P_{dis,s,t} \tag{14}$$

$$PFR_{s,t} \leq \frac{\Delta f^{max} - DB_t}{R_s^{eq}} \tag{15}$$

$$(1 - \lambda_{s,t})Dis_s^{min} \leq P_{dis,s,t}/\eta \leq (1 - \lambda_{s,t})Dis_s^{max} \tag{16}$$

$$P_{dis,s,t}^{Energy} + AGC_{s,t}^{up} \leq P_{dis,s,t} \tag{17}$$

$$P_{ch,s,t}^{Energy} - AGC_{s,t}^{down} = P_{ch,s,t} \tag{18}$$

$$Chi_s^{min}\lambda_{s,t} \leq P_{ch,s,t}\eta \leq Chi_s^{max}\lambda_{s,t} \tag{19}$$

$$Chi_s^{min}\lambda_{s,t} \leq P_{ch,s,t}^{Energy}\eta \leq Chi_s^{max}\lambda_{s,t} \tag{20}$$

The total ancillary service requirements are calculated with a percentage of the IEM load. Note that RTED also permits ancillary service shortages:

$$\sum PFR_{i,t} \geq PFR_t^{req} \cdot \sum P_{L,j,t} - PFR_t^{short} \tag{21}$$

$$\sum AGC_{i,t}^{up} \geq AGC_{up,t}^{req} \cdot \sum P_{L,j,t} - AGC_{up,t}^{short} \tag{22}$$

$$\sum AGC_{i,t}^{down} \geq AGC_{down,t}^{req} \cdot \sum P_{L,j,t} - AGC_{down,t}^{short} \tag{23}$$

where PFR_t^{short}, $AGC_{up,t}^{short}$ and $AGC_{down,t}^{short}$ are the ancillary service shortage variables.

D. The single-phase power system model

We formulate the optimal power flow constraints based on the single-phase branch flow model [3].

$$\sum_{l\in\Omega(j)} H_{l,t} - \sum_{l\in\Pi(j)} (H_{l,t} - R_l l_{l,t}) = P_{g,j,t} + (dis_{j,t}^{Energy} - ch_{j,t}^{Energy}) - (P_{L,j,t} - DR_{j,t}) \tag{24}$$

$$\sum_{l\in\Omega(j)} G_{l,t} - \sum_{l\in\Pi(j)} (G_{l,t} - X_l l_{l,t}) = Q_{G,j,t} - Q_{L,j,t} \tag{25}$$

$$u_{j,t} = u_{i,t} - 2(R_l H_{l,t} + X_l G_{l,t}) + (R_l^2 + X_l^2) l_{l,t} \tag{26}$$

$$H_{l,t}^2 + G_{l,t}^2 = l_{l,t} u_{i,t} \tag{27}$$

$$H_{l,t}^2 + G_{l,t}^2 \le S_l^2 \tag{28}$$

$$0 \le DR_{j,t} \le P_{L,j}^{DR} \tag{29}$$

$$u_j^{min,2} \le u_{j,t} \le u_j^{max,2} \tag{30}$$

where $u_{i,t} = |V_{i,t}|^2$ and $l_{l,t} = |I_{l,t}|^2$ are squared amplitudes of nodal voltage and line current; $H_{l,t}$ and $G_{l,t}$ indicate the active and reactive power flow on line l; R_l and X_l are line impedance. (24)-(25) are the energy balance constraints; (26)-(28) are line constraints; (29) constrains demand responses; (30) is voltage constraint. The nonlinear constraint (31) can be relaxed by SOCP, yielding:

$$H_{l,t}^2 + G_{l,t}^2 \le l_{l,t} u_{i,t} \tag{31}$$

E. The gas system model

The gas flow model includes the gas demand balance (32), gas nodal pressure limits (33), gas retailer capacity constraint (34), compressor ratio constraint (35), gas flow limit (36) and in/out-flow relationship (37).

$$g_{gm,t}^{gr} - \sum_{gl\in\Pi(gm)} gf_{gl,t}^{c,in} + \sum_{gl\in\Omega(gm)} gf_{gl,t}^{c,out} - \sum_{gl\in\Pi(gm)} gf_{gl,t} + \sum_{gl\in\Omega(gm)} gf_{gl,t} = dis_{gm,t} - ch_{gm,t} + GD_{gm,t} + p_{g,t}\beta_g \tag{32}$$

$$\pi_{gm,t}^{min} \le \pi_{gm,t} \le \pi_{gm,t}^{max} \tag{33}$$

$$g_{gm,t}^{gr} \le G_{gm}^{max} \tag{34}$$

$$\pi_{gn,t} \le \gamma_c \pi_{gm,t} \tag{35}$$

$$gf_{gl,t}^{min} \le gf_{gl,t} \le gf_{gl,t}^{max} \tag{36}$$

$$(1-\alpha_c) gf_{gf,t}^{in} = gf_{gf,t}^{out} \tag{37}$$

$$gf_{gl,t}^2 = \theta_l(\pi_{gm,t}^2 - \pi_{gn,t}^2) \tag{38}$$

where $g_{gm,t}^{gr}$ is the natural gas procured from the gas retailer; $gf_{gl,t}^{c,in}, gf_{gl,t}^{c,out}$, and $gf_{gl,t}$ are the gas flow variables on inactive pipelines and compressors. The gas-fired DG's consumption is formulated as a gas load with conversion coefficient β_g. In the gas system, the Weymouth function (38) describes the relationship between nodal gas pressure and gas flow through a pipeline. It is the source of non-convexity, and we will formulate a SOCP relaxation for the Weymouth function. To relax this function by SOCP, the equality constraint can be relaxed into inequality constraint:

$$gf_{gl,t}^2 \le \theta_l(\pi_{gm,t}^2 - \pi_{gn,t}^2) \tag{39}$$

This relaxation for natural gas flow is usually tight for integrated electricity-natural gas systems [4].

F. The heat system model

We simplify the heat system with a CHP generator and a heat load node. The feasible region of the heat and electric power provided by a CHP unit can be illustrated by the convex polyhedron shown in Fig. 1. Denoting $N_{chp} = 1, 2, .., N$, the heat and electric power generated by a CHP unit can be formulated as a set of linear constraints:

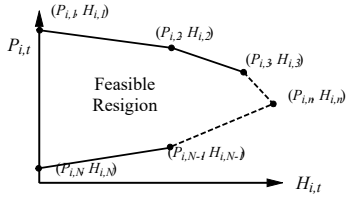

Fig. 1. Feasible operation region of a CHP unit.

$$h_{i,t} = h_{i,t}^{load} \tag{40}$$

$$h_{i,t} = \sum_{n\in N_{chp}} \zeta_{i,t}^n H_{i,n} \tag{41}$$

$$P_{i,t} = \sum_{n\in N_{chp}} \zeta_{i,t}^n P_{i,n} \tag{42}$$

$$\sum_{n\in N_{chp}} \zeta_{i,t} = 1, \zeta \ge 0 \tag{43}$$

With coefficients C_i, E_i and J_i, the operation cost of a CHP unit is usually formulated as:

$$f_{i,t}^{CH} = C_i^a P_{i,t}^2 + C_i^b P_{i,t} + C_i^c + E_i^a h_{i,t}^2 + E_i^b h_{i,t} + E_i^c + J_i P_{i,t} h_{i,t} \tag{44}$$

According to [5], (44) can be approximated by a set of lower linear functions. Given $M \times N$ points $(P_i^m, h_i^n, f_i^{m,n})$, (44) is approximated by the following linear constraints:

$$f_{i,t}^{CH} \ge \partial P_i^{m,n}(P_{i,t} - P_i^m) + \partial h_i^{m,n}(h_{i,t} - h_i^n) + f_i^{m,n} \tag{45}$$

$$\partial P_i^{m,n} = 2C_i^a P_i^m + C_i^b + J_i h_i^n \tag{46}$$

$$\partial h_i^{m,n} = 2E_i^a P_i^m + E_i^b + J_i P_i^m \tag{47}$$

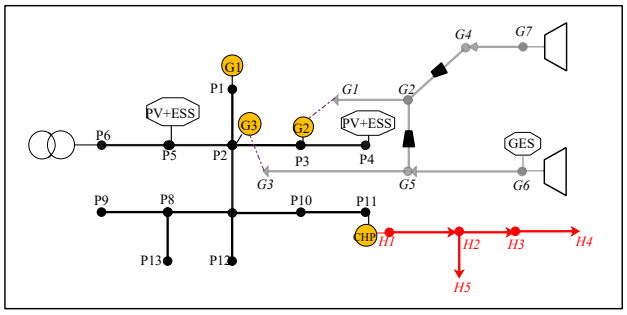

Fig. 2. Test system topology.

III. Case Studies

The proposed RTED model is tested on a test system consisting of 13 power nodes, 7 gas nodes and 5 heat nodes, shown in Fig. 2. The detailed description of the test systems can be found in [8]. The RTED is run every 15 minutes for 24 hours. At every run, the rolling-horizon look-ahead window is 3 hours, of T=12 intervals.

In the RTED, we assume that the day-ahead unit commitment signals indicate that all DGs are on. The result of RTED is summarized in TABLE I. Three cases are tested:

- Case 1: ESSs and GESs are functional and ESSs can provide ancillary services;
- Case 2: ESSs and GESs are not installed in the test system;
- Case 3: ESSs and GESs are functional, but ESSs does not provide ancillary services.

TABLE I
Costs of Three Cases

Cost	Case 1 ($)	case 2 ($)	Case 3 ($)
Overall	23115.18	24618.63	23759.62
Power	-261.36	1179.30	383.075
Gas	9885.40	9948.18	9885.40
Heat	13491.14	13491.14	13491.14

TABLE II
Costs of the Power System Operation

Cost	Case 1 ($)	case 2 ($)	Case 3 ($)
Non-gas	618.66	618.66	618.66
Buy-grid	1047.67	1122.74	856.59
Sell-grid	-2875.92	-2620.63	-3228.07
ESS	66.59	0	61.35
DR	601.18	577.11	590.90
Lineloss	280.40	277.16	279.37
Ancillary shortage	0.02	1204.25	1204.25

Case 1 is the base case. The overall cost of one day's operation is $23115.18, among which $9885.40 is from the gas system, $13491.14 is from the heat system, and the power system makes a revenue of $261.36. The specific share of each component from the power system costs is listed in TABLE II. Case 1 can provide most ancillary services.

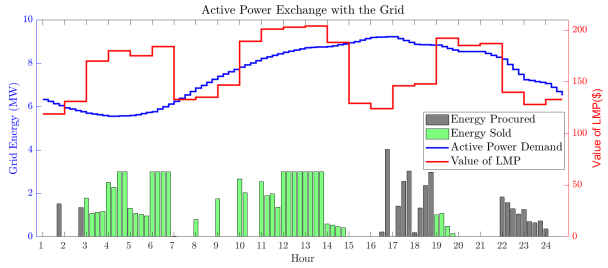

Fig. 3. The Energy Exchange with the Main Grid.

It is straightforward that leveraging ESSs in the IEM could increase the systems well-being, as Case 1 has 6.11% lower cost than Case 2. While energy storage is functional, the IEM can procure energy from the main grid when the price is low and store the energy in ESSs, then when the price goes high, ESSs release the stored energy and make economic benefits, as shown in the difference between the energy procurement and energy sold in Fig. 3 and this is the main income of the power distribution system. Similarly, for the gas distribution system, there is also a volatility in the gas retail price, which enables the profitability of GESs, as is shown in Fig. 4. The charging and discharging profiles of ESSs and GESs are presented in Fig. 5.

The generation costs of non-gas DG in three cases are the same, as the generation unit is willing to be fully dispatched and sell more power to make profits, as shown in Fig. 6. The power output from CHP is correlated with the heat production, so to satisfy the heat demand, a certain level of power output has to be maintained. The cost of the heat system for all the cases are the same.

For ancillary service provision, the benefit of enabling ESSs to provide ancillary services is demonstrated by case 1 and case 3, where an additional ancillary shortage penalty is incurred. The ancillary service profiles are presented in Fig. 7. The ancillary service capability of each DG is limited by the ramp rate, so if ESSs cannot provide ancillary services, the ancillary service shortage penalty will occur.

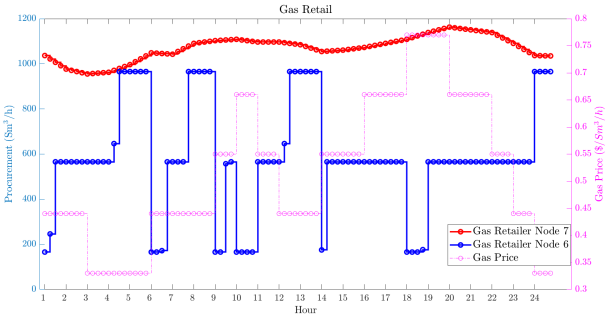

Fig. 4. Gas Price and Gas Procurement.

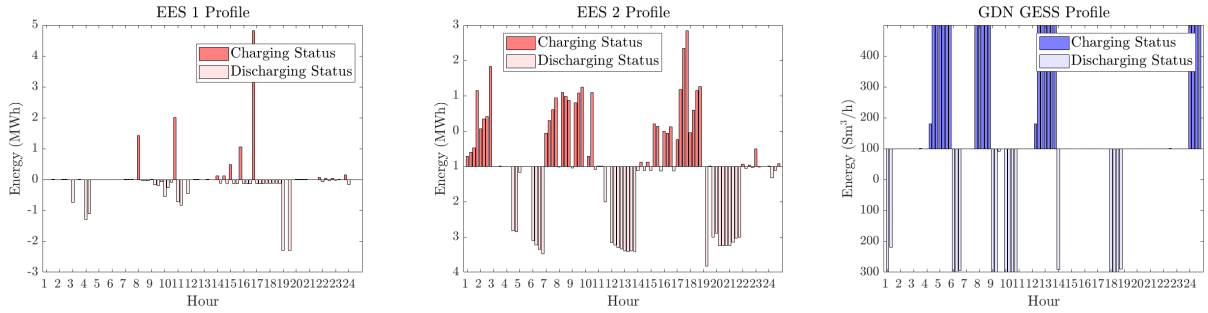

(a) (b) (c)

Fig. 5. The Profile of ESS and GES.

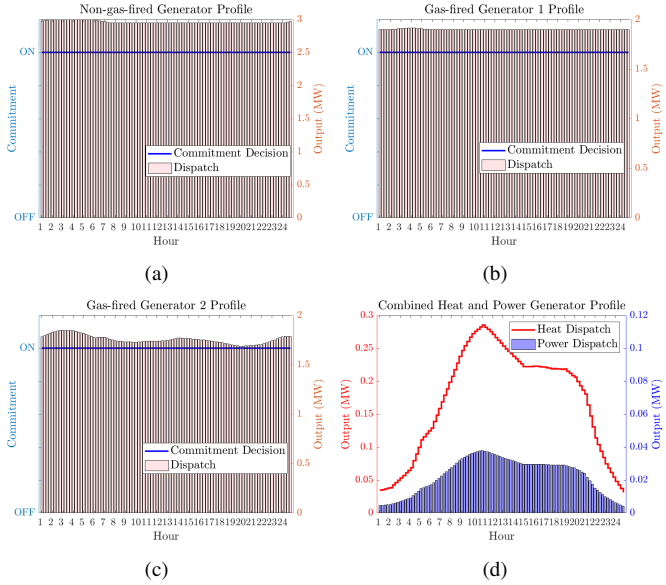

(a) (b) (c) (d)

Fig. 6. The DG output.

IV. Conclusion

In conclusion, due to the increasing interdependence among the energy systems, RTED is essential to ensure the safe and economic operation of the IEM. To bridge the existing works with the practical issues from the integrated energy system, this paper proposes the appropriate energy flow models for individual energy systems, integrates the ancillary requirements, and establishes the optimization problem for the integrated energy system RTED.

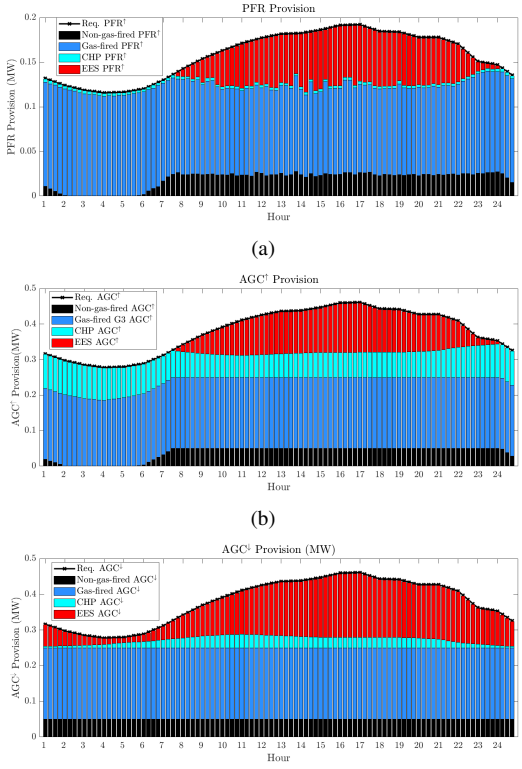

(a) (b) (c)

Fig. 7. The Profile of Ancillary services.

References

[1] Y. Zhang, J. Wang, and Z. Li, "Uncertainty modeling of distributed energy resources: techniques and challenges," *Curr. Sustain. Energy Rep.*, vol. 6, no. 2, pp. 4251, June 2019.

[2] Z. Tang and B. Akin, "Suppression of dead-time distortion through revised repetitive controller in PMSM Drives,"*IEEE Trans. Energy Convers.* , vol. 32, no. 3, pp. 918-930, 2017.

[3] T. Ding, Y. Lin, Z. Bie, and C. Chen,"A resilient microgrid formation strategy for load restoration considering master-slave distributed generators and topology reconfiguration." *Applied energy*, vol. 199, pp.205-216, 2017.

[4] Y. He, M. Shahidehpour, Z. Li, C. Guo and B. Zhu, "Robust Constrained Operation of Integrated Electricity-Natural Gas System Considering Distributed Natural Gas Storage," *IEEE Transactions on Sustainable Energy*, vol. 9, no. 3, pp. 1061-1071, July 2018.

[5] B. Liu, K. Meng, Z. Dong and W. Wei, "Optimal Dispatch of Coupled Electricity and Heat System With Independent Thermal Energy Storage," *IEEE Transactions on Power Systems*, vol. 34, no. 5, pp. 3250-3263, Jul 2019.

[6] B. Xu , Y. Dvorkin , D. S. Kirschen, . C. A. S. C. A. Silva-Monroy and J.-P. Watson, "A comparison of policies on the participation of storage in U.S. frequency regulation markets," in *2016 IEEE Power and Energy Society General Meeting (PESGM)*, Boston, MA, USA, 2016.

[7] Y. Wang, C. Wan, Z. Zhou, K. Zhang and A. Botterud, "Improving Deployment Availability of Energy Storage With Data-Driven AGC Signal Models," *IEEE Transactions on Power Systems*, vol. 33, no. 4, pp. 4207-4217, July 2018.

[8] https://sites.google.com/view/yanlinglin/data/integrated-energy-system.